



Published in final edited form as:

Toxicol Lett. 2017 January 15; 266: 32–41. doi:10.1016/j.toxlet.2016.11.019.

Tetrabromobisphenol A activates the hepatic interferon pathway in rats

J.K. Dunnick^{a,*}, D.L. Morgan^b, S.A. Elmore^c, K. Gerrish^d, A. Pandiri^c, T.V. Ton^c, K.R. Shockley^e, and B.A. Merrick^f

^aToxicology Branch, National Institute of Environmental Health Sciences, Research Triangle Park, NC, USA

^bNTP Laboratory, National Institute of Environmental Health Sciences, Research Triangle Park, NC, USA

^cCellular and Molecular Pathology, National Institute of Environmental Health Sciences, Research Triangle Park, NC, USA

^dMolecular Genomics Core, National Institute of Environmental Health Sciences, Research Triangle Park, NC, USA

^eBiostatistics and Computational Biology Branch, National Institute of Environmental Health Sciences, Research Triangle Park, NC, USA

^fBiomolecular Screening Branch, National Institute of Environmental Health Sciences, Research Triangle Park, NC, USA

Abstract

Tetrabromobisphenol A (TBBPA) is a widely used flame retardant in printed circuit boards, paper, and textiles. In a two-year study, TBBPA showed evidence of uterine tumors in female Wistar-Han rats and liver and colon tumors in B6C3F1 mice. In order to gain further insight into early gene and pathway changes leading to cancer, we exposed female Wistar Han rats to TBBPA at 0, 25, 250, or 1000 mg/kg (oral gavage in corn oil, 5×/week) for 13 weeks. Because at the end of the TBBPA exposure period, there were no treatment-related effects on body weights, liver or uterus lesions, and liver and uterine organ weights were within 10% of controls, only the high dose animals were analyzed. Analysis of the hepatic and uterine transcriptomes showed TBBPA-induced changes primarily in the liver (1000 mg/kg), with 159 transcripts corresponding to 132 genes differentially expressed compared to controls (FDR = 0.05). Pathway analysis showed activation of interferon (IFN) and metabolic networks. TBBPA induced few molecular changes in the uterus. Activation of the interferon pathway in the liver occurred after 13-weeks of TBBPA exposure, and with longer term TBBPA exposure this may lead to immunomodulatory changes that contribute to carcinogenic processes.

*Corresponding author. dunnickj@niehs.nih.gov (J.K. Dunnick).

Conflict of interest

There is no conflict of interest.

Appendix A. Supplementary data

Supplementary data associated with this article can be found, in the online version, at <http://dx.doi.org/10.1016/j.toxlet.2016.11.019>.

Keywords

Tetrabromobisphenol A; Toxicogenomics; Microarray; Interferon response transcripts; Pathway analysis

1. Introduction

Tetrabromobisphenol A (TBBPA) is a high production volume brominated flame retardant (Malkoske et al., 2016), used in printed circuit boards, paper, and textiles (U. S. EPA, 2015; Zhou et al., 2014). TBBPA exposure occurs from breast milk (Carignan et al., 2012; Harrad and Abdallah, 2015; Nakao et al., 2015), food ingestion (e.g. fish (Svihlikova et al., 2015)), industrial exposures (Zhou et al., 2014), dust in the home (Di Napoli-Davis and Owens, 2013), and at waste sites (Liu et al., 2016). TBBPA also accumulates in marine life and may be toxic to various fish species (He et al., 2015; Tang et al., 2015).

TBBPA caused clear evidence of uterine adenocarcinomas in female Wistar Han rats [CrI:WI(Han)] in a 2-year study (Dunnick et al., 2015; National Toxicology Program, 2014). These TBBPA-induced uterine tumors were highly malignant with metastases to the liver, pancreas, kidney, thyroid and other organ systems. Other TBBPA carcinogenic findings occurred in the liver, lower intestine, and vascular systems of male mice (National Toxicology Program, 2014). TBBPA has been classified as probably carcinogenic to humans (Group 2a) by the Interagency for Research on Cancer (IARC) based on sufficient evidence for carcinogenicity found in the 2-year rodent studies and mechanistic information reported in the literature (Grosse et al., 2016).

In this study we looked for TBBPA-induced transcriptomic changes in the liver because this organ is a primary site for metabolism of hormones and other chemicals (Tsuchiya et al., 2005), and in the uterus, a target site for TBBPA-induced tumors in rats (National Toxicology Program, 2014). The TBBPA carcinogenic effect in the uterus is of concern because endometrial tumors are a common malignancy in women with an estimated 50,000 new cases per year in the U.S. (Siegel et al., 2013), and one million new cases per year worldwide (Webb, 2015). Uterine cancer is predicted to be one of the three leading cancers in women by 2030 (Rahib et al., 2014). The majority of human uterine tumors are endometrial carcinomas (George et al., 2015); the same type of uterine tumors seen in rats after TBBPA exposure (National Toxicology Program, 2014). Environmental factors are thought to play a role in the development of uterine cancer (Lichtenstein et al., 2000), including chemical and hormone effects (e.g. tamoxifen and estrogen) (IARC, 2012).

TBBPA is a nongenotoxic chemical, and toxicokinetic studies of TBBPA in the female rat did not reveal any specific accumulation of the parent compound or metabolites in the uterus (compared to that in other organ systems) (Knudsen et al., 2014). Thus, these 13-week TBBPA studies were undertaken to identify molecular alterations in the liver and/or uterus to help characterize early changes along the pathway to cancer.

2. Materials and methods

2.1. Experimental design

Tetrabromobisphenol A (CAS No. 79-94-7; Albemarle Corporation (Baton Rouge, LA), lot M032607 K) (Fig. 1) was prepared for oral gavage administration in corn oil to deliver TBBPA at doses of 0, 25, 250, or 1000 mg/kg body weight in a volume of 5 mL/kg body weight. Female Wistar Han IGS rats (CrI:WI(Han)) (25 animals/dose level) were obtained from Charles River (Raleigh, NC). 1000 mg/kg was a dose at which TBBPA induced uterine tumors in the female rat (National Toxicology Program, 2014), and transcriptomic patterns of liver and uterus were examined at this dose level. Two lower doses were added (25 and 250 mg/kg) to examine the uterus for transcriptomic changes, because this was the target organ in the 2-year cancer study. At the start of the study the animals were 5–6 weeks of age. The animals were housed two per cage. Tap water and NTP-2000 diet (Zeigler Brothers, Inc. Gardners, PA) were made available for ad libitum consumption.

Body weights were obtained at one day prior to dosing and weekly thereafter. The treatment schedule was five days per week, excluding weekends and holidays, for up to 13 weeks. Animals were treated for a minimum of two consecutive days (within 24 h) prior to necropsy. Animals were not treated on the morning of scheduled sacrifice. At sacrifice, animals were euthanized with CO₂. At necropsy uterine and liver organ weights were taken, and uterine and liver samples fixed in formalin for histopathologic evaluation at all dose levels. Sections were taken from the uterus (control and all dose levels) and liver (control and high dose) and flash frozen for the molecular studies.

The uterus with horns, vagina, and ovaries were harvested. The ovaries and vagina from each animal were fixed in formalin. The uterus was weighed then transected along the midline, including uterine body, such that one half of the uterus (including horn and body) was flash frozen in liquid nitrogen for RNA extraction. The other half of the uterus (including horn and body) was laid out, stretched with minimal tension, and pinned onto a piece of heavy card stock and placed in formalin. This was to prevent curling and shrinkage of the uterine body and horn so that it could be trimmed longitudinally without curling. This allowed appropriate microscopic interpretation of any changes.

The liver was removed and weighed, and then approximately a one-gram sample of the left lobe was collected and minced into approximately 3 mm cubes while on a weigh boat sitting in dry ice. The cubes were then frozen in liquid nitrogen in the weigh boat and, once frozen, transferred to three labeled, 2.0 mL cryotubes and flash frozen in liquid nitrogen. The liver samples were collected and frozen within 5 min of each animal's sacrifice. An adjacent section (~3 mm) of the remaining left lobe of the liver was collected and placed in a labeled cassette and fixed in formalin for histopathology.

The care of animals on this study was according to NIH procedures as described in the “The U.S. Public Health Service Policy on Humane Care and Use of Laboratory Animals”, available from the Office of Laboratory Animal Welfare, National Institutes of Health, Department of Health and Human Services, RKL1, Suite 360, MSC 7982, 6705 Rockledge Drive, Bethesda, MD 20892-7982 or online at <http://grants.nih.gov/grants/olaw/>

[olaw.htm#pol](#). The protocol was approved by the laboratory where the animals were housed and dosed (Alion Science and Technology Animal Care and Use Committee).

2.2. Uterine and liver RNA preparation and microarray hybridization

A section of the frozen liver and one half of the frozen uterus (flash frozen and stored at -80°C) were placed into RNAlater[®] (Ambion, Inc., Austin, TX). RNA was extracted from control and treated liver and uterus to identify any molecular changes at a dose that caused uterine tumors (1000 mg/kg). RNA extraction was performed on tissues from 15 to 16 randomly selected animals per group.

RNA was extracted from the flash frozen uterine or liver tissues using the Invitrogen PureLink Mini kit (Invitrogen cat# 12183-018A, Carlsbad, CA) according to the manufacturer's protocol. Frozen tissue samples were lysed and homogenized in TRIzol reagent (Invitrogen) using a rotor-stator homogenizer. Isolation of RNA was performed according to the mini kit protocol. On-column deoxyribonuclease (DNase) treatment was performed using the Invitrogen PureLink DNase kit (Invitrogen) to purify the RNA samples. RNA concentration and quality were measured on a Bioanalyzer (Agilent Technologies, Santa Clara, CA). Samples were aliquoted and stored at -80°C until they were analyzed.

Total RNA was used to synthesize double-stranded cDNA for each sample using Affymetrix GeneChip[®] Expression Analysis with 3' amplification two-cycle target labeling and control reagents (Affymetrix Inc. Santa Clara, CA). The cDNA served as a template to synthesize biotin-labeled antisense cRNA using an in vitro transcription (IVT) labeling kit. Labeled cRNA was fragmented and hybridized to the Affymetrix Rat Genome 230 2.0 Genechip[®] Array. Array hybridization, washing, and staining were performed according to the Affymetrix recommended protocol EuKGE_Ws2v5. The chips were scanned using an Affymetrix GeneChip[®] Scanner 3000. Quality control measurements were evaluated to determine if the data derived from the arrays were of sufficient quality prior to comparisons for differential expression.

2.3. Microarray data analysis

Gene expression analysis was conducted using Affymetrix Rat Genome 230 2.0 GeneChip[®] arrays (Affymetrix, Santa Clara, CA). Total RNA was amplified as directed in the Affymetrix 3' IVT Plus kit protocol. 15 μg of amplified biotin-aRNAs were fragmented and 12.5 μg were hybridized to each array for 16 h at 45°C in a rotating hybridization oven using the Affymetrix Eukaryotic Target Hybridization Controls and protocol. Array slides were stained with streptavidin/phycoerythrin utilizing a double-antibody staining procedure and then washed for antibody amplification according to the GeneChip[®] Hybridization, Wash and Stain Kit and user manual. Arrays were scanned in an Affymetrix Scanner 3000 and data was obtained using the GeneChip[®] Command Console and Expression Console Software (AGCC; Version 3.2 and Expression Console; Version 1.2).

2.4. Data normalization

Probe intensity data from all Rat Genome 230 version 2 Affymetrix GeneChip[®] arrays were read into the R software environment (<http://www.R-project.org>) directly from. CEL files

using the R/affy package (Gautier et al., 2004). Probe-level data quality was assessed using image reconstruction, histograms of raw signal intensities and hierarchical clustering of samples. Normalization was carried out using the robust multi-array average (RMA) method using all probe intensity data sets together (Irizarry et al., 2003). The RMA method adjusts the background intensities of perfect match (PM) probes, applies quantile normalization, and calculates final expression measures using the Tukey median polish algorithm. RMA scatterplots were used as an additional quality control measure.

2.5. Statistical assessment of differential gene expression

Gene expression between control and treated liver and uterine samples was evaluated for each probe set using a bootstrap *t*-test approach. Pairwise tests were conducted while controlling the false discovery rate (FDR) at the 5% level. All statistical calculations were performed in the ORIOGEN software package using 10,000 bootstrap samples (Peddada et al., 2005).

Ingenuity Pathway Analysis database (www.ingenuity.com) was used to compare experimental gene expression signatures to thousands of genomic signatures derived from published microarray data sets. This data mining approach is based on rank-based statistical procedures and is analogous to the Gene Set Enrichment method (Subramanian et al., 2005).

The upstream regulator analysis presented here is based on known relationships between transcriptional factor molecules and targets stored in the Ingenuity Knowledge Base. For each transcription factor, an overlap *p*-value is used to compare the overlap between the number of known transcription factor targets and the number of targets found in the TBBPA gene list. The activation *z*-score is used to compare the activation state of each transcription factor as described in the literature with the direction of change in TBBPA expression relative to control samples that are found in the current study. In addition, the interferome database (www.interferome.org) was used to identify significant transcripts in the interferon pathway (Rusinova et al., 2013).

2.6. Nanostring analysis

Microarray results were confirmed using the nCounter platform by NanoString© (www.nanostring.com) utilizing a Custom Code-Set consisting of 10 TBBPA responsive genes that were significantly altered by about 2-fold from control after microarray analysis. Genes evaluated by Nanostring were *Agri*, *Mx1*, *Mx2*, *Irf7*, *Usp18*, *Oas1a*, *Oas1b*, *Sng*, *Tsx*, and *Usp18*, using the housekeeping genes *Gapdh*, *Hprt1*, *Med15* and *Rpl7* for normalization. For liver samples in Nanostring analysis, 100 ng of amplified cDNA, obtained utilizing the Nugen™ Ovation Pico WTA System (v2), was used. Gene expression was quantified on the nCounter Digital Analyzer™ and raw and normalized counts were generated with nSolver (v2.5)™ software. All data passed nSolver 's QA/QC.

2.7. Infection screening

Sentinel animals were randomly selected for parasite evaluation, gross observation for evidence of disease, and serum collection for serology at 4 weeks after receipt (5 rats) and at the end of the study (5 rats). Sentinels were from the vendor's same animal room as the

experimental rats and were subjected to the same environmental conditions. Serum samples were shipped to an independent laboratory (Idexx BioResearch, Columbia, MO) for bacterial and viral titer testing. Serum was tested for antibodies to *Mycoplasma pulmonis*, RPV, RMV, KRV, H1, PMV, RCV/SDAV, RTV, and Sendai virus. All tests were negative.

3. Results

3.1. Body and organ weights and histopathologic findings

There was little or no treatment-related toxicity after 13 weeks of TBBPA exposure using conventional toxicity endpoints. This included no treatment-related effects on survival, body weight, or organ weights (Table 1). There were no treatment-related microscopic lesions in the liver or uterus.

3.2. Liver transcriptomic alterations

Using a false discovery rate threshold of 0.05, there were 159 differentially expressed liver transcript probes (Table 2). These 159 transcripts corresponded to expression level changes in 132 genes (6 genes were identified by two probes; Supplement 1). The heat map of these TBBPA liver transcript patterns showed a clear difference between control and TBBPA treated liver (Fig. 2).

Nanostring analysis of selected transcripts confirmed the direction of the TBBPA-induced transcript change (Fig. 3), although *Agrn* and *Sncg* were minimally responsive to TBBPA by Nanostring analysis. Selected liver transcript signals were plotted by individual animals to display variance of control and TBBPA groups. Generally, transcript responses showed the same elevated direction of response of TBBPA treatment group compared to control (Fig. 4).

Ingenuity Pathway enrichment analysis provided evidence that the interferon (IFN) pathway was the most significant pathway affected by TBBPA treatment (Table 3). This led us to explore the IFN pathway more closely. There were 59 significantly altered TBBPA hepatic transcripts in the IFN pathway (www.interferome.org). Transcripts altered by TBBPA that are known to play critical roles in the interferon pathway included *Irf-7*, *Mx1*, *Oas1*, *Isgf15*, *Ddx60*, *Stat1* and *Stat2*. Also upregulated were TBBPA transcripts involved in liver xenobiotic metabolism, including genes regulating fatty acid metabolism (*Scd2*, *Cyp2b6*, *Elovl6*, *Herc6*, *Fasn*) (Table 2).

There were few TBBPA-induced changes in the uterine transcriptome. Using a false discovery rate threshold of 0.05, there were 4 differentially expressed transcripts at 1000 mg/kg, 8 at 250 mg/kg, and 5 at 25 mg/kg. All 17 transcripts at various dose levels were less than 1.5 fold changed versus control uterine transcript expression levels. None of the 17 uterine transcripts were common among the three TBBPA exposure levels examined (25, 250, and 1000 mg/kg), and none overlapped the 138 TBBPA liver transcripts found to be altered (1000 mg/kg). These transcript changes were not considered to alter organ function.

4. Discussion

In this study we found that TBBPA induced molecular changes in the liver after 13-weeks of exposure (1000 mg/kg), while there were few altered transcripts in the uterus. TBBPA caused liver expression changes in 159 significant Affymetrix probes (relative to controls [FDR = 0.05]) which mapped to 132 genes. The TBBPA hepatic transcriptome included transcripts with functions in the IFN pathway (Noureddin et al., 2015; Sathish and Yuan, 2011; Schmeisser et al., 2010; Schneider et al., 2014) and in xenobiotic and fatty acid metabolism.

The TBBPA hepatic transcripts included upregulation of *Scd2* (sterol-coenzyme A desaturase 2), *Elovl-6* (fatty acid elongase 6), and *Fasn* (fatty acid synthase). *Scd2* is a crucial enzyme in the synthesis of monounsaturated fatty acids which are required for maintaining a normal epidermal permeability barrier function, and are components of triglycerides (Miyazaki et al., 2005). Alterations in *Scd2* levels may affect lipid content in non-hepatic organs (de Moura et al., 2016) where level and type of lipid is critical to function. *Elovl-6* is one of six mammalian enzymes responsible for fatty acid elongation beyond 16 carbons to produce very long chain fatty acids. The *FASN* enzyme catalyzes de novo synthesis of fatty acids (Dorn et al., 2010). TBBPA also increased levels of the *Cyp2b6*, a transcript induced by phenobarbital and in xenobiotic metabolism (Liu et al., 2015). The expression of *Cyp2b6* can have a 20–250 fold inter-individual variation (Wang and Tompkins, 2008). Because liver is a major site for chemical exposure (Hakk et al., 2000; Knudsen et al., 2014; Kuester et al., 2007) and is involved in estradiol metabolism (Gosavi et al., 2013; Raftogianis et al., 2000), these TBBPA-induced liver changes could affect hormone levels.

TBBPA induced IFN pathway transcripts (www.interferome.org) previously identified in liver cells (Rusinova et al., 2013). This included transcripts associated with IFN pathway regulation (e.g. *Stat1*, *Stat2*, *Ilf7*, *Irf9*, *Pml*) (Khodarev et al., 2012); antiviral activity (e.g. *Mx1*, *Mx2*, *Ift3*, *Isg15*); and regulation of immune response (*DDX58*, *Oas1*) (Hertzog et al., 2011). Some of the TBBPA IFN pathway transcripts (e.g. *Isg15*) may be involved in hepatic cancer (Li et al., 2014), and could also play a role in the liver cancer that occurred in mice in the 2-year TBBPA study (National Toxicology Program, 2014). *Il127* (induced by TBBPA) may promote cell proliferation (Hsieh et al., 2015), and is associated with tumorigenesis and invasion (Li et al., 2015).

Like TBBPA, tamoxifen causes uterine tumors (IARC, 2012), and induces interferon pathway transcripts (e.g. *MX1* and interferon regulatory factors) in model systems (Dabydeen et al., 2015; Fawzy et al., 2012; Schild-Hay et al., 2009). Exposure of myeloid cells to a related chemical, bisphenol A, also stimulated interferon signaling (Panchanathan et al., 2015). These TBBPA findings are supported by recent in vitro studies which showed TBBPA alterations in IFN production in human cells (Almughamsi and Whalen, 2016).

While TBBPA has little activity as an estrogen receptor agonist or antagonist (Hamers et al., 2006), a feedback loop between estrogen signaling and IFN signaling has been reported (Panchanathan et al., 2015, 2010). Upregulation of interferon pathways by TBBPA and

tamoxifen could affect estrogen signaling and ultimately the development of uterine cancer. The ability of TBBPA to interact with sulfotransferase (Gosavi et al., 2013) could disrupt estrogen homeostasis (Sanders et al., 2016). In addition, TBBPA can cause oxidative damage and disruption of thyroid hormone signaling (He et al., 2016; Iakovleva et al., 2016). Further work is needed to determine how these various TBBPA effects work together to cause cancer and how age affects biologic outcome (Hines, 2008).

Decreases in immune function can facilitate cancer development (Yang and Rosenberg, 2016), and in several studies TBBPA was found to suppress the immune system. TBBPA was an immunosuppressant in in vitro cell systems including suppression of NK cell activity (Hurd and Whalen, 2011; Kibakaya et al., 2009). Mice treated with TBBPA were less able to mount a defense against viral infection (Watanabe et al., 2010). Interferon signaling modulates immune activity, and *Irf7* when upregulated in the liver, as occurred in these TBBPA studies (Fig. 5), can regulate the immune system (Wang et al., 2013). Persistent IFN signaling can disrupt immune responsiveness potentially leading to immune suppression (Teijaro, 2016). This TBBPA immunosuppressant activity was thought to contribute to its carcinogenic properties in a recent review of TBBPA studies (Grosse et al., 2016).

One interpretation of the TBBPA-mediated IFN signature reported in our study might be as a general stress response to repeated chemical exposure. The expression of 'IFN stimulated genes' or 'interferon signaling network genes' (ISGs) in response to various viral, bacterial and chemical stimuli has been well characterized and described (de Veer et al., 2001; Schneider et al., 2014). In our studies animals were screened for a broad spectrum of infections and none were found, suggesting that the IFN pathway activation was not due to microbial or viral exposure. In addition, liver histopathology showed no overt signs of cell death or organ damage. Exactly, how TBBPA-mediated expression of ISGs in liver might influence or contribute to uterine carcinogenesis is unclear at this time. Although blood cytokine measurements were not performed in this study, it is possible that TBBPA could alter circulating or organ-localized production of interferon to affect ISGs leading to the IFN signature observed here in liver. For example, microarray analysis in an independent study showed that acute pentachlorophenol exposure in C57BL/6 mice increased expression of many interferon responsive transcripts in liver, including *Stat1*, *Stat2*, *Irf7*, *Oas*, *Ifit* as well as other IFN regulated genes (Kanno et al., 2013). These authors proposed a scheme where pentachlorophenol produced metabolites and oxygenated radicals leading to DNA and protein damage that resulted in pathway activation of the Nrf2/Tir receptor and PRR (pattern response recognition) systems to initiate interferon signaling and expression of ISGs. Another study found in vitro TBBPA exposure disrupted IFN- γ secretion from various human immune cell preparations (Almughamsi and Whalen, 2016). Whether the uterus would respond similarly to TBBPA or other chemical exposures and engage IFN-dependent pathways is an untested hypothesis. IFN polymorphisms are associated with increased risk of cervical cancer (Sun et al., 2015) but the relationship of IFN-related mechanisms with uterine carcinogenesis requires further investigation.

In summary, conventional biochemical and toxicological measures and histologic lesions were not observed in either liver or uterus in female Wistar Han rats after 13 weeks of repeated TBBPA exposure from 25 to 1000 mg/kg. Toxicogenomic analysis showed no

substantial changes in uterus but did reveal a robust gene expression in liver that involved activation of the interferon pathway. We speculate that long-term TBBPA exposures could lead to direct or indirect immunomodulatory changes that contribute to carcinogenic processes in the uterus.

Supplementary Material

Refer to Web version on PubMed Central for supplementary material.

Acknowledgments

This research was supported [in part] by the Intramural Research Program of the NIH, National Institute of Environmental Health Sciences. We thank M. Cesta, NIEHS, and G. Knudson, NCI for their review of this manuscript.

References

- Almughamsi H, Whalen MM. Hexabromocyclododecane and tetrabromobisphenol A alter secretion of interferon gamma (IFN-gamma) from human immune cells. *Arch. Toxicol.* 2016; 90(7):1695–1707. [PubMed: 26302867]
- Carignan CC, Abdallah MA, Wu N, Heiger-Bernays W, McClean MD, Harrad S, Webster TF. Predictors of tetrabromobisphenol-A (TBBP-A) and hexabromocyclododecanes (HBCD) in milk from Boston mothers. *Environ. Sci. Technol.* 2012; 46(21):12146–12153. [PubMed: 22998345]
- Dabydeen SA, Kang K, Diaz-Cruz ES, Alamri A, Axelrod ML, Bouker KB, Al-Kharboosh R, Clarke R, Hennighausen L, Furth PA. Comparison of tamoxifen and letrozole response in mammary preneoplasia of ER and aromatase overexpressing mice defines an immune-associated gene signature linked to tamoxifen resistance. *Carcinogenesis.* 2015; 36(1):122–132. [PubMed: 25421723]
- Di Napoli-Davis G, Owens JE. Quantitation of tetrabromobisphenol-A from dust sampled on consumer electronics by dispersed liquid–liquid microextraction. *Environ. Pollut.* 2013; 180:274–280. [PubMed: 23792388]
- Dorn C, Riener MO, Kirovski G, Saugspier M, Steib K, Weiss TS, Gabele E, Kristiansen G, Hartmann A, Hellerbrand C. Expression of fatty acid synthase in nonalcoholic fatty liver disease. *Int. J. Clin. Exp. Pathol.* 2010; 3(5):505–514. [PubMed: 20606731]
- Dunnick JK, Sanders JM, Kissling GE, Johnson CL, Boyle MH, Elmore SA. Environmental chemical exposure may contribute to uterine cancer development: studies with tetrabromobisphenol A. *Toxicol. Pathol.* 2015; 43(4):464–473. [PubMed: 25476797]
- Fawzy IO, Negm M, Ahmed R, Esmat G, Hamdi N, Abdelaziz AI. Tamoxifen alleviates hepatitis C virus-induced inhibition of both toll-like receptor 7 and JAK-STAT signalling pathways in PBMCs of infected Egyptian females. *J. Viral Hepat.* 2012; 19(12):854–861. [PubMed: 23121363]
- Gautier L, Cope L, Bolstad BM, Irizarry RA. affy-analysis of Affymetrix GeneChip data at the probe level. *Bioinformatics.* 2004; 20(3):307–315. [PubMed: 14960456]
- George SM, Ballard R, Shikany JM, Crane TE, Neuhouser ML. A prospective analysis of diet quality and endometrial cancer among 84,415 postmenopausal women in the women's health initiative. *Ann. Epidemiol.* 2015; 25(10):788–793. [PubMed: 26260777]
- Gosavi RA, Knudsen GA, Birnbaum LS, Pedersen LC. Mimicking of estradiol binding by flame retardants and their metabolites: a crystallographic analysis. *Environ. Health Perspect.* 2013; 121(10):1194–1199. [PubMed: 23959441]
- Grosse Y, Loomis D, Guyton KZ, El Ghissassi F, Bouvard V, Benbrahim-Tallaa L, Mattock H, Straif K. Carcinogenicity of some industrial chemicals. *Lancet Oncol.* 2016; 17(4):419–420. [PubMed: 26928709]

- Hakk H, Larsen G, Bergman A, Orn U. Metabolism, excretion and distribution of the flame retardant tetrabromobisphenol-A in conventional and bile-duct cannulated rats. *Xenobiotica*. 2000; 30(9): 881–890. [PubMed: 11055266]
- Hamers T, Kamstra JH, Sonneveld E, Murk AJ, Kester MH, Andersson PL, Legler J, Brouwer A. In vitro profiling of the endocrine-disrupting potency of brominated flame retardants. *Toxicol. Sci*. 2006; 92(1):157–173. [PubMed: 16601080]
- Harrad S, Abdallah MA. Concentrations of polybrominated diphenyl ethers, hexabromocyclododecanes and tetrabromobisphenol-A in Breast milk from United Kingdom women do not decrease over twelve months of lactation. *Environ. Sci. Technol*. 2015; 49(23): 13899–13903. [PubMed: 25924207]
- He Q, Wang X, Sun P, Wang Z, Wang L. Acute and chronic toxicity of tetrabromobisphenol A to three aquatic species under different pH conditions. *Aquat. Toxicol*. 2015; 164:145–154. [PubMed: 25980965]
- He M, Li X, Zhang S, Sun J, Cao H, Wang W. Mechanistic and kinetic investigation on OH-initiated oxidation of tetrabromobisphenol A. *Chemosphere*. 2016; 153:262–269. [PubMed: 27018518]
- Hertzog P, Forster S, Samarajiwa S. Systems biology of interferon responses. *J. Interferon Cytokine Res*. 2011; 31(1):5–11. [PubMed: 21226606]
- Hines RN. The ontogeny of drug metabolism enzymes and implications for adverse drug events. *Pharmacol. Ther*. 2008; 118(2):250–267. [PubMed: 18406467]
- Hsieh WL, Huang YH, Wang TM, Ming YC, Tsai CN, Pang JH. IFI27, a novel epidermal growth factor-stabilized protein, is functionally involved in proliferation and cell cycling of human epidermal keratinocytes. *Cell Prolif*. 2015; 48(2):187–197. [PubMed: 25664647]
- Hurd T, Whalen MM. Tetrabromobisphenol A decreases cell-surface proteins involved in human natural killer (NK) cell-dependent target cell lysis. *J. Immunotoxicol*. 2011; 8(3):219–227. [PubMed: 21623697]
- International Agency for Research on Cancer (IARC). IARC monographs on the evaluation of carcinogenic risks to humans. *Pharmaceuticals: A review of human carcinogens*. Vol. 101A. IARC; Lyon, France: 2012.
- Iakovleva I, Begum A, Brannstrom K, Wijsekera A, Nilsson L, Zhang J, Andersson PL, Sauer-Eriksson AE, Olofsson A. Tetrabromobisphenol A is an efficient stabilizer of the transthyretin tetramer. *PLoS One*. 2016; 11(4):e0153529. [PubMed: 27093678]
- Irizarry RA, Hobbs B, Collin F, Beazer-Barclay YD, Antonellis KJ, Scherf U, Speed TP. Exploration, normalization, and summaries of high density oligonucleotide array probe level data. *Biostatistics*. 2003; 4(2):249–264. [PubMed: 12925520]
- Kanno J, Aisaki K, Igarashi K, Kitajima S, Matsuda N, Morita K, Tsuji M, Moriyama N, Furukawa Y, Otsuka M, Tachihara E, Nakatsu N, Kodama Y. Oral administration of pentachlorophenol induces interferon signaling mRNAs in C57BL/6 male mouse liver. *J. Toxicol. Sci*. 2013; 38(4):643–654. [PubMed: 23892564]
- Khodarev NN, Roizman B, Weichselbaum RR. Molecular pathways: interferon/stat1 pathway: role in the tumor resistance to genotoxic stress and aggressive growth. *Clin. Cancer Res*. 2012; 18(11): 3015–3021. [PubMed: 22615451]
- Kibakaya EC, Stephen K, Whalen MM. Tetrabromobisphenol A has immunosuppressive effects on human natural killer cells. *J. Immunotoxicol*. 2009; 6(4):285–292. [PubMed: 19908946]
- Knudsen GA, Sanders JM, Sadik AM, Birnbaum LS. TETRABROMOBISPHENOL A disposition and kinetics of tetrabromobisphenol A in female Wistar han rats. *Toxicol. Rep*. 2014; 1:214–223. [PubMed: 24977115]
- Kuester RK, Solyom AM, Rodriguez VP, Sipes IG. The effects of dose, route, and repeated dosing on the disposition and kinetics of tetrabromobisphenol A in male F-344 rats. *Toxicol. Sci*. 2007; 96(2):237–245. [PubMed: 17234645]
- Li C, Wang J, Zhang H, Zhu M, Chen F, Hu Y, Liu H, Zhu H. Interferon-stimulated gene 15 (ISG15) is a trigger for tumorigenesis and metastasis of hepatocellular carcinoma. *Oncotarget*. 2014; 5(18): 8429–8441. [PubMed: 25238261]

- Li S, Xie Y, Zhang W, Gao J, Wang M, Zheng G, Yin X, Xia H, Tao X. Interferon alpha-inducible protein 27 promotes epithelial-mesenchymal transition and induces ovarian tumorigenicity and stemness. *J. Surg. Res.* 2015; 193(1):255–264. [PubMed: 25103640]
- Lichtenstein P, Holm NV, Verkasalo PK, Iliadou A, Kaprio J, Koskenvuo M, Pukkala E, Skytthe A, Hemminki K. Environmental and heritable factors in the causation of cancer—analyses of cohorts of twins from Sweden, Denmark, and Finland. *N. Engl. J. Med.* 2000; 343(2):78–85. [PubMed: 10891514]
- Liu Z, Li L, Wu H, Hu J, Ma J, Zhang QY, Ding X. Characterization of CYP2B6 in a CYP2B6-humanized mouse model: inducibility in the liver by phenobarbital and dexamethasone and role in nicotine metabolism in vivo. *Drug Metab. Dispos.* 2015; 43(2):208–216. [PubMed: 25409894]
- Liu K, Li J, Yan S, Zhang W, Li Y, Han D. A review of status of tetrabromobisphenol A (TBBPA) in China. *Chemosphere.* 2016; 148:8–20. [PubMed: 26800486]
- Malkoske T, Tang Y, Xu W, Yu S, Wang H. A review of the environmental distribution, fate, and control of tetrabromobisphenol A released from sources. *Sci. Total Environ.* 2016
- Miyazaki M, Dobrzyn A, Elias PM, Ntambi JM. Stearoyl-CoA desaturase-2 gene expression is required for lipid synthesis during early skin and liver development. *Proc. Natl. Acad. Sci. U. S. A.* 2005; 102(35):12501–12506. [PubMed: 16118274]
- Nakao T, Akiyama E, Kakutani H, Mizuno A, Aozasa O, Akai Y, Ohta S. Levels of tetrabromobisphenol A, tribromobisphenol A, dibromobisphenol A, monobromobisphenol A, and bisphenol a in Japanese breast milk. *Chem. Res. Toxicol.* 2015; 28(4):722–728. [PubMed: 25719948]
- National Toxicology Program. Toxicology studies of tetrabromobisphenol A (Cas no. 79–94-7) in F344/NTac rats and B6C3F1/N mice and toxicology and carcinogenesis studies of tetrabromobisphenol A in Wistar Han [CrI:WI (Han)] rats and B6C3F1/N mice. NTP Technical Report 587. 2014
- Noureddin M, Rotman Y, Zhang F, Park H, Rehmann B, Thomas E, Liang TJ. Hepatic expression levels of interferons and interferon-stimulated genes in patients with chronic hepatitis C: A phenotype-genotype correlation study. *Genes Immun.* 2015; 16(5):321–329. [PubMed: 26020282]
- Panchanathan R, Shen H, Zhang X, Ho SM, Choubey D. Mutually positive regulatory feedback loop between interferons and estrogen receptor-alpha in mice: implications for sex bias in autoimmunity. *PLoS One.* 2010; 5(5):e10868. [PubMed: 20526365]
- Panchanathan R, Liu H, Leung YK, Ho SM, Choubey D. Bisphenol A (BPA) stimulates the interferon signaling and activates the inflammasome activity in myeloid cells. *Mol. Cell. Endocrinol.* 2015; 415:45–55. [PubMed: 26277401]
- Peddada S, Harris S, Zajd J, Harvey E. ORIOGEN: an order restricted inference for ordered gene expression data. *Bioinform.* 2005; 21:3933–3934.
- Raftogianis R, Creveling C, Weinshilboum R, Weisz J. Estrogen metabolism by conjugation. *J. Natl. Cancer Inst. Monogr.* 2000; 27:113–124.
- Rahib L, Smith BD, Aizenberg R, Rosenzweig AB, Fleshman JM, Matrisian LM. Projecting cancer incidence and deaths to 2030: the unexpected burden of thyroid, liver, and pancreas cancers in the United States. *Cancer Res.* 2014; 74(11):2913–2921. [PubMed: 24840647]
- Rusinova I, Forster S, Yu S, Kannan A, Masse M, Cumming H, Chapman R, Hertzog PJ. Interferome v2.0: an updated database of annotated interferon-regulated genes. *Nucleic Acids Res.* 2013; 41:D1040–D1046. (Database issue). [PubMed: 23203888]
- Sanders JM, Coulter SJ, Knudsen GA, Dunnick JK, Kissling GE, Birnbaum LS. Disruption of estrogen homeostasis as a mechanism for uterine toxicity in Wistar Han rats treated with tetrabromobisphenol A. *Toxicol. Appl. Pharmacol.* 2016; 298:31–39. [PubMed: 26988606]
- Sathish N, Yuan Y. Evasion and subversion of interferon-mediated antiviral immunity by Kaposi's sarcoma-associated herpesvirus: an overview. *J. Virol.* 2011; 85(21):10934–10944. [PubMed: 21775463]
- Schild-Hay LJ, Leil TA, Divi RL, Olivero OA, Weston A, Poirier MC. Tamoxifen induces expression of immune response-related genes in cultured normal human mammary epithelial cells. *Cancer Res.* 2009; 69(3):1150–1155. [PubMed: 19155303]

- Schmeisser H, Mejido J, Balinsky CA, Morrow AN, Clark CR, Zhao T, Zoon KC. Identification of alpha interferon-induced genes associated with antiviral activity in Daudi cells and characterization of IFIT3 as a novel antiviral gene. *J. Virol.* 2010; 84(20):10671–10680. [PubMed: 20686046]
- Schneider WM, Chevillotte MD, Rice CM. Interferon-stimulated genes: a complex web of host defenses. *Annu. Rev. Immunol.* 2014; 32:513–545. [PubMed: 24555472]
- Siegel R, Naishadham D, Jemal A. Cancer statistics, 2013. *CA cancer. J. Clin.* 2013; 63(1):11–30. [PubMed: 23335087]
- Subramanian A, Tamayo P, Mootha VK, Mukherjee S, Ebert BL, Gillette MA, Paulovich A, Pomeroy SL, Golub TR, Lander ES, Mesirov JP. Gene set enrichment analysis: a knowledge-based approach for interpreting genome-wide expression profiles. *Proc. Natl. Acad. Sci. U. S. A.* 2005; 102(43): 15545–15550. [PubMed: 16199517]
- Sun Y, Lu Y, Pen Q, Li T, Xie L, Deng Y, Qin A. Interferon gamma +874T/A polymorphism increases the risk of cervical cancer: evidence from a meta-analysis. *Tumour Biol.* 2015; 36(6):4555–4564. [PubMed: 25649976]
- Svihlikova V, Lankova D, Poustka J, Tomaniova M, Hajslova J, Pulkrabova J. Perfluoroalkyl substances (PFASs) and other halogenated compounds in fish from the upper Labe river basin. *Chemosphere.* 2015; 129:170–178. [PubMed: 25455680]
- Tang B, Zeng YH, Luo XJ, Zheng XB, Mai BX. Bioaccumulative characteristics of tetrabromobisphenol A and hexabromocyclododecanes in multi-tissues of prey and predator fish from an e-waste site, South China. *Environ. Sci. Pollut. Res. Int.* 2015
- Tejaro JR. Type I interferons in viral control and immune regulation. *Curr. Opin. Virol.* 2016; 16:31–40. [PubMed: 26812607]
- Tsuchiya Y, Nakajima M, Yokoi T. Cytochrome P450-mediated metabolism of estrogens and its regulation in human. *Cancer Lett.* 2005; 227(2):115–124. [PubMed: 16112414]
- U. S. EPA. Fame retardants in printed circuit boards. <http://www.epa.gov/OTS0574261>. 2015. (<http://www2.epa.gov/saferchoice/design-environment-alternatives-assessments>)
- Wang H, Tompkins LM. CYP2B6: new insights into a historically overlooked cytochrome P450 isozyme. *Curr. Drug Metab.* 2008; 9(7):598–610. [PubMed: 18781911]
- Wang XA, Zhang R, Zhang S, Deng S, Jiang D, Zhong J, Yang L, Wang T, Hong S, Guo S, She ZG, Zhang XD, Li H. Interferon regulatory factor 7 deficiency prevents diet-induced obesity and insulin resistance. *Am. J. Physiol. Endocrinol. Metab.* 2013; 305(4):E485–495. [PubMed: 23695216]
- Watanabe W, Shimizu T, Sawamura R, Hino A, Konno K, Hirose A, Kurokawa M. Effects of tetrabromobisphenol A, a brominated flame retardant, on the immune response to respiratory syncytial virus infection in mice. *Int. Immunopharmacol.* 2010; 10(4):393–397. [PubMed: 20074668]
- Webb PM. Environmental (nongenetic) factors in gynecological cancers: update and future perspectives. *Future Oncol.* 2015; 11(2):295–307.
- Yang JC, Rosenberg SA. Adoptive T-Cell therapy for cancer. *Adv. Immunol.* 2016; 130:279–294. [PubMed: 26923004]
- Zhou X, Guo J, Zhang W, Zhou P, Deng J, Lin K. Tetrabromobisphenol A contamination and emission in printed circuit board production and implications for human exposure. *J. Hazard. Mater.* 2014; 273C:27–35.
- de Moura RF, Nascimento LF, Ignacio-Souza LM, Morari J, Razolli DS, Solon C, de Souza GF, Festuccia WT, Velloso LA. Hypothalamic stearoyl-CoA desaturase-2 (SCD2) controls whole-body energy expenditure. *Int. J. Obes. (Lond.)*. 2016; 40(3):471–478. [PubMed: 26392016]
- de Veer MJ, Holko M, Frevel M, Walker E, Der S, Paranjape JM, Silverman RH, Williams BR. Functional classification of interferon-stimulated genes identified using microarrays. *J. Leukoc. Biol.* 2001; 69(6):912–920. [PubMed: 11404376]

HIGHLIGHTS

- Tetrabromobisphenol A (TBBPA) is a widely used flame retardant.
- Oral administration of TBBPA to rats cause transcriptomic changes in the liver.
- These transcriptomic changes indicated activation of the interferon pathway.

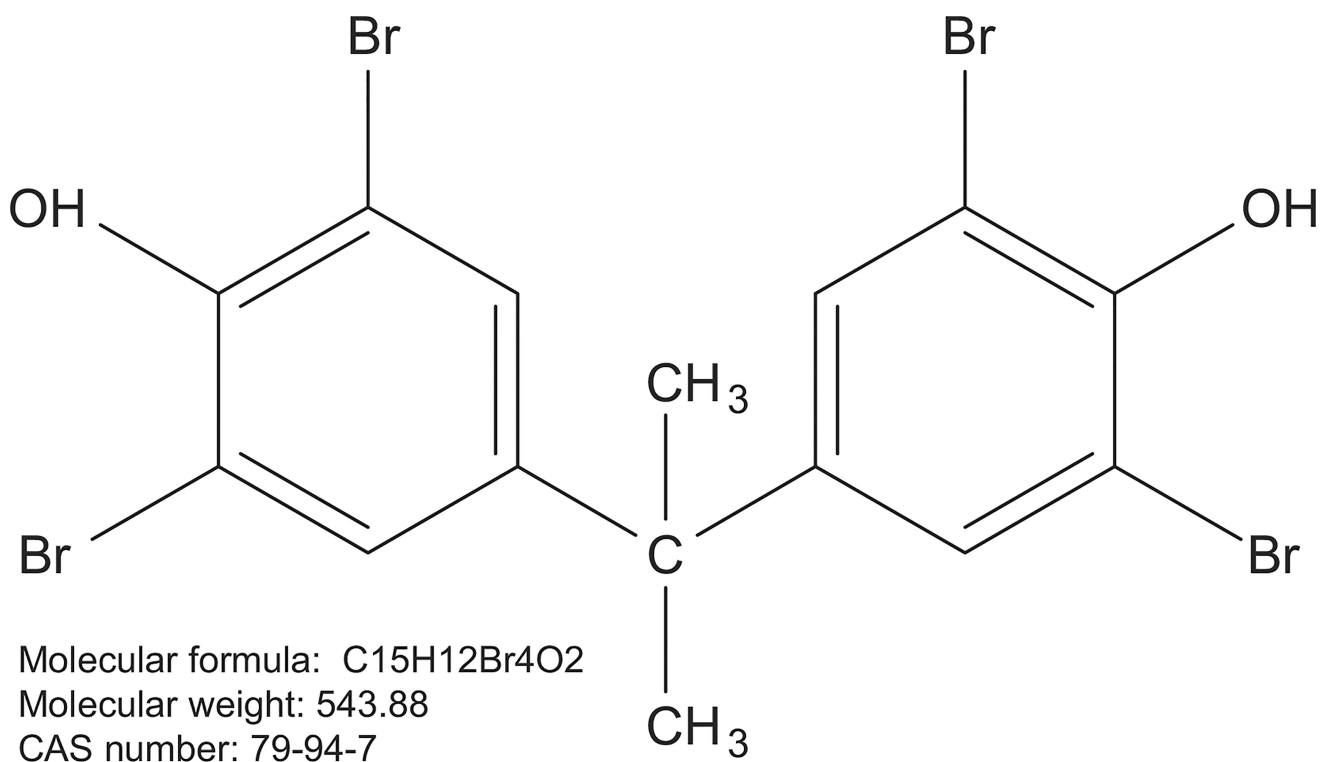


Fig. 1.
TBPPA structure.

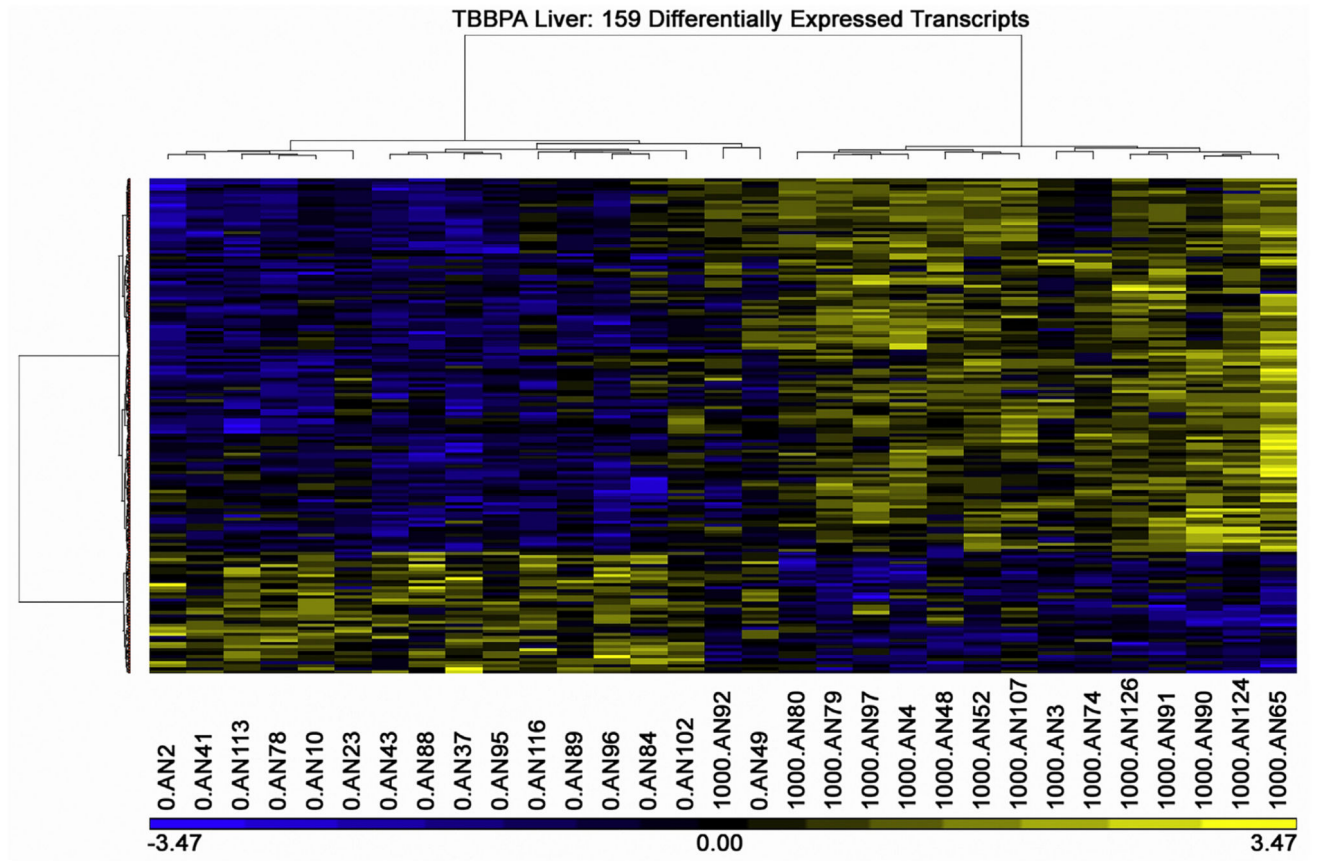


Fig. 2.
TBBPA (1000 mg/kg) liver transcript heat map.

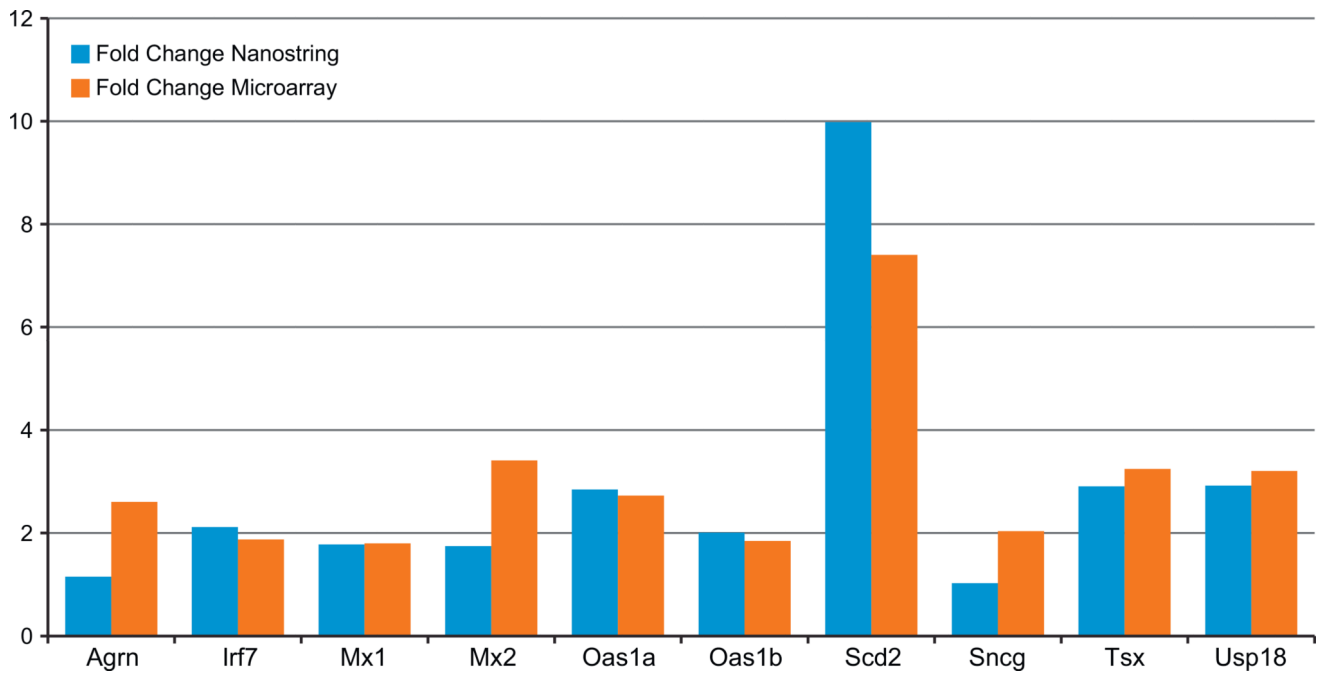


Fig. 3.
Selected Liver TBBPA (1000 mg/kg) transcripts confirmed by Nanostring analysis.

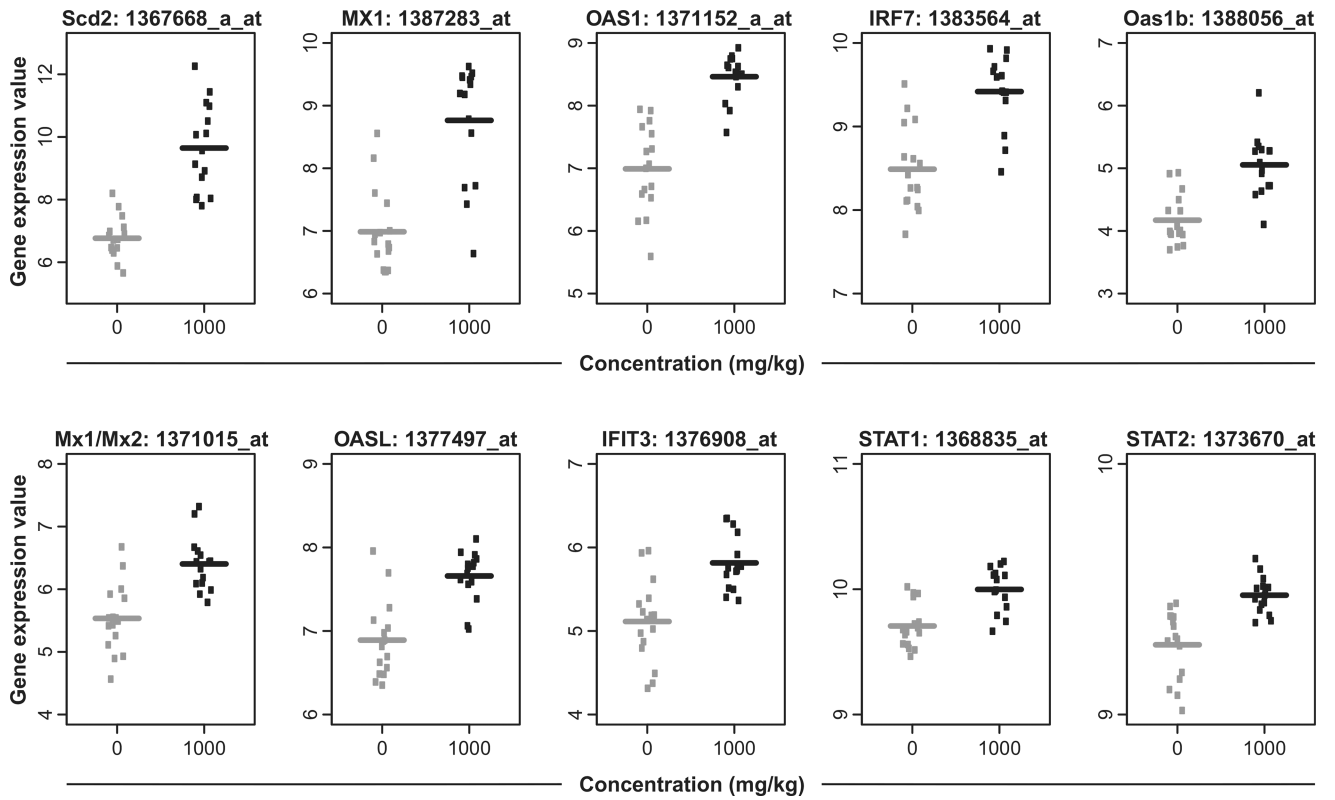


Fig. 4. Plots of selected TBBPA (1000 mg/kg) induced-liver transcripts. The gene expression value shown refers to the RMA normalized gene expression measure described in the methods.

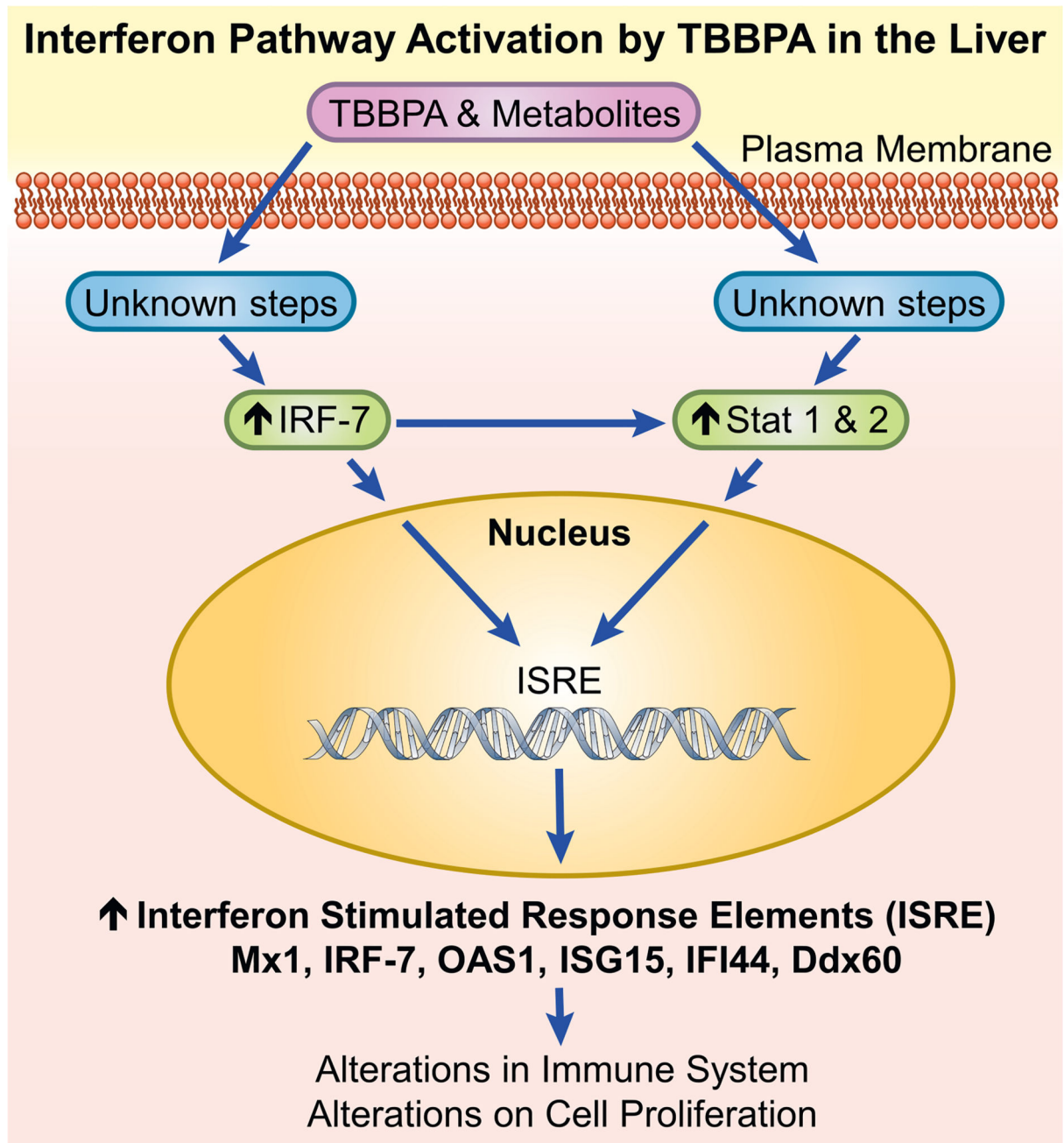


Fig. 5.
Proposed Mechanism for TBBPA activation of interferon pathway.

Table 1
Body weight, liver, and uterus weight in female Wistar Han rats after 13-weeks of TBBPA dosing.

Dose (mg/kg)	Terminal Body wt. (g)	Liver wt. (g)	Relative Liver Weight	Uterus wt (g)	Relative Uterus Wt.	N
0	241.7 ± 3.704	8.13 ± 0.190	33.55 ± 0.563	0.92 ± 0.081	3.87 ± 0.362	22-23
25	230.6 ± 3.435	7.74 ± 0.143	33.60 ± 0.427	1.07 ± 0.077	4.65 ± 0.31	25
250	236.1 ± 4.148	7.89 ± 0.1	33.45 ± 0.411	0.97 ± 0.070	4.14 ± 0.309	24
1000	244.6 ± 3.036	8.71 ± 0.11*	35.63 ± 0.29**	0.97 ± 0.06	3.99 ± 0.286	21

Relative organ weight = organ weight/body weight.

* p < 0.05.

** p < 0.01.

Table 2

TBBPA-induced liver transcripts after 13-weeks of TBBPA dosing (1000 mg/kg).

Fold Change	ID	Symbol	Entrez Gene Name
7.363	1367668_a_at	Scd2	stearoyl-Coenzyme A desaturase 2
3.428	1387283_at	MX18	MX dynamin-like GTPase 1
3.264	1389034_at	USP18*	ubiquitin specific peptidase 18
3.065	1368736_at	Tsx	testis specific X-linked gene
2.773	1371152_a_at	OAS18	2'-5'-oligoadenylate synthetase 1, 40/46 kDa
2.633	1382314_at	*	ISG15 ubiquitin-like modifier
2.258	1371076_at	CYP2B6	cytochrome P450, family 2, subfamily B, polypeptide 6
2.199	1394401_at	ELOVL6	ELOVL fatty acid elongase 6
2.189	1382902_at	HERC6*	HECT and RLD domain containing E3 ubiquitin protein ligase family member 6
1.939	1379748_at	IFI44L*	interferon-induced protein 44-like
1.904	1383564_at	IRF7*	interferon regulatory factor 7
1.844	1388056_at	Oas1b	2'-5' oligoadenylate synthetase 1B
1.833	1381556_at	Ddx60*	DEAD (Asp-Glu-Ala-Asp) box polypeptide 60
1.827	1369698_at	ABCC3*	ATP-binding cassette, sub-family C (CFTR/MRP), member 3
1.826	1371015_at	Mx1/Mx2*	MX dynamin-like GTPase 1
1.734	1387137_at	COMP	cartilage oligomeric matrix protein
1.703	1377497_at	OASL*	2'-5'-oligoadenylate synthetase-like
1.666	1367707_at	FASN	fatty acid synthase
1.658	1370913_at	RSAD2*	radical S-adenosyl methionine domain containing 2
1.627	1376908_at	IFIT3*	interferon-induced protein with tetratricopeptide repeats 3
1.565	1381960_at	ROPN1L	rhophilin associated tail protein 1-like
1.543	1381206_at	PLCXD2	phosphatidylinositol-specific phospholipase C, X domain containing 2
1.527	1383424_at	CMPK2*	cytidine monophosphate (UMP-CMP) kinase 2, mitochondrial
1.500	1390127_at	DIXDC1	DIX domain containing 1
1.490	1391507_at	ZNF4678	zinc finger protein 467
1.486	1370379_at	PRSS8	protease, serine, 8
1.468	1376920_at	LOC500013	similar to sterile alpha motif domain containing 9-like
1.462	1388164_at	HLA-E	major histocompatibility complex, class I, E
1.459	1391754_at	LOC100910735/Oas1i	2' - 5' oligoadenylate synthetase 1i
1.455	1379656_a_at	CORO2A	coronin, actin binding protein, 2A
1.451	1373267_at	SH3YL1	SH3 and SYLF domain containing 1
1.433	1383357_a_at	RELL1	RELT-like 1
1.421	1383448_at	IRF98	interferon regulatory factor 9
1.415	1367854_at	ACLY*	ATP citrate lyase
1.408	1381014_at	IFI44*	interferon-induced protein 44
1.407	1367708_a_at	FASN*	fatty acid synthase
1.378	1378581_at	CCDC62	coiled-coil domain containing 62

Fold Change	ID	Symbol	Entrez Gene Name
1.350	1391702_at	ZNF446*	zinc finger protein 446
1.349	1371694_at	DPYSL2	dihydropyrimidinase-like 2
1.346	1369716_s_at	Lgals5	lectin, galactose binding, soluble 5
1.332	1390312_at	LOC684193	similar to sterile alpha motif domain containing 9-like
1.328	1385252_at	TRIM6-TRIM34	TRIM6-TRIM34 readthrough
1.320	1393044_at	CMPK2	cytidine monophosphate (UMP-CMP) kinase 2, mitochondrial
1.314	1380071_at	PARP12*	poly (ADP-ribose) polymerase family, member 12
1.299	1373514_at	RNF213*	ring finger protein 213
1.287	1388152_at	MAP2*	microtubule-associated protein 2
1.269	1388979_at	SMNDC1	survival motor neuron domain containing 1
1.266	1373506_at	FAM102A	family with sequence similarity 102, member A
1.247	1371901_at	DDHD2	DDHD domain containing 2
1.247	1391463_at	Ddx588	DEAD (Asp-Glu-Ala-Asp) box polypeptide 58
1.245	1390641_at	ZNF346	zinc finger protein 346
1.237	1377878_at	FGFBP3	fibroblast growth factor binding protein 3
1.236	1372705_at	CHERP	calcium homeostasis endoplasmic reticulum protein
1.225	1374337_at	RNF2138	ring finger protein 213
1.224	1368835_at	STAT1*	signal transducer and activator of transcription 1, 91 kDa
1.222	1370803_at	ZWINT8	ZW10 interacting kinetochore protein
1.220	1373090_at	SSR1	signal sequence receptor, alpha
1.215	1397764_at	KCTD5	potassium channel tetramerization domain containing 5
1.215	1389883_at	TMEM65	transmembrane protein 65
1.212	1383621_at	MBTPS2	membrane-bound transcription factor peptidase, site 2
1.211	1372930_at	SP110*	SP110 nuclear body protein
1.210	1373288_at	ST5*	suppression of tumorigenicity 5
1.203	1376339_at	WWC3*	WWC family member 3
1.200	1398435_at	SLC22A15*	solute carrier family 22, member 15
1.199	1371996_at	AEBP2	AE binding protein 2
1.198	1372779_at	B3GNT2*	UDP-GlcNAc:betaGal beta-1,3-N-acetylglucosaminyltransferase 2
1.198	1383034_at	Rybp*	RING1 and YY1 binding protein
1.195	1367693_at	YWHAH	tyrosine 3-monooxygenase/tryptophan 5-monooxygenase activation protein, eta
1.194	1395081_at	NCOA7*	nuclear receptor coactivator 7
1.187	1399157_at	URI1	URI1, prefoldin-like chaperone
1.184	1369559_a_at	CD47*	CD47 molecule
1.180	1369978_at	PRPSAP2	phosphoribosyl pyrophosphate synthetase-associated protein 2
1.177	1382540_at	PRPF40A	PRP40 pre-mRNA processing factor 40 homolog A (S. cerevisiae)
1.174	1394761_at	ARHGAP42	Rho GTPase activating protein 42
1.172	1374482_at	CTPS2	CTP synthase 2
1.172	1382177_at	PML*	promyelocytic leukemia
1.169	1383158_at	AGFG1	ArfGAP with FG repeats 1

Fold Change	ID	Symbol	Entrez Gene Name
1.168	1380960_at	CORO2A	coronin, actin binding protein, 2A
1.167	1388997_at	ARF3	ADP-ribosylation factor 3
1.166	1387770_at	Ifi27*	interferon, alpha-inducible protein 27
1.163	1384362_at	ZBTB24	zinc finger and BTB domain containing 24
1.159	1375431_at	C2orf69	chromosome 2 open reading frame 69
1.157	1370244_at	CTSV*	cathepsin V
1.156	1374815_at	STARD3NL	STARD3 N-terminal like
1.155	1389686_at	PRKX	protein kinase, X-linked
1.152	1373563_at	SNRNP27	small nuclear ribonucleoprotein 27 kDa (U4/U6.U5)
1.151	1376492_at	UNKL	unkempt family zinc finger-like
1.150	1392916_at	MAP7	microtubule-associated protein 7
1.148	1370351_at	TDRD78	tudor domain containing 7
1.147	1379669_at	ARHGAP42	Rho GTPase activating protein 42
1.147	1373670_at	STAT2*	signal transducer and activator of transcription 2, 113 kDa
1.146	1389646_at	CDC23	cell division cycle 23
1.142	1388930_at	TMEM123	transmembrane protein 123
1.131	1372360_at	ABI1	abl-interactor 1
1.128	1390387_at	SH3D19	SH3 domain containing 19
1.119	1374637_at	TMCO6	transmembrane and coiled-coil domains 6
1.115	1374707_at	CCAR2	cell cycle and apoptosis regulator 2
1.113	1374406_at	KLHDC2*	kelch domain containing 2
1.112	1384022_at	AGFG1	ArfGAP with FG repeats 1
1.104	1368217_at	RALBP1*	ralA binding protein 1
1.101	1373974_at	OSBP	oxysterol binding protein
1.099	1375639_at	E2F6	E2F transcription factor 6
1.080	1384971_at	DEPDC7	DEP domain containing 7
-1.102	1383244_at	IQCE*	IQ motif containing E
-1.122	1393123_at	C8G	complement component 8, gamma polypeptide
-1.125	1369898_a_at	GIP	gastric inhibitory polypeptide
-1.137	1371916_at	MSRB*	methionine sulfoxide reductase B1
-1.137	1380624_at	VANGL1	VANGL planar cell polarity protein 1
-1.145	1370682_at	LILRA6*	leukocyte immunoglobulin-like receptor, subfamily A (with TM domain), member 6
-1.146	1376761_at	HDAC4	histone deacetylase 4
-1.152	1370202_at	PLA2G16*	phospholipase A2, group XVI
-1.156	1368399_a_at	CPQ*	carboxypeptidase Q
-1.160	1370853_at	CAMK2N1	calcium/calmodulin-dependent protein kinase II inhibitor 1
-1.160	1370267_at	GSK3B	glycogen synthase kinase 3 beta
-1.168	1376410_at	MMP17	matrix metalloproteinase 17 (membrane-inserted)
-1.170	1398351_at	USP7	ubiquitin specific peptidase 7 (herpes virus-associated)
-1.174	1367586_at	Ldha/RGD1562690	lactate dehydrogenase A

Fold Change	ID	Symbol	Entrez Gene Name
-1.176	1377112_at	CDA*	cytidine deaminase
-1.194	1399070_at	SETD5	SET domain containing 5
-1.199	1372490_at	GPD1L*	glycerol-3-phosphate dehydrogenase 1-like
-1.207	1368190_at	REN	renin
-1.220	1383989_at	SOX4*	SRY (sex determining region Y)-box 4
-1.222	1372195_at	TNNC2*	troponin C type 2 (fast)
-1.245	1396188_at	RHOJ	ras homolog family member J
-1.253	1381193_at	LPGAT1*	lysophosphatidylglycerol acyltransferase 1
-1.253	1374048_at	NRTN	neurturin
-1.263	1370375_at	GLS2	glutaminase 2 (liver, mitochondrial)
-1.292	1393949_at	HYAL3	hyaluronoglucosaminidase 3
-1.293	1382981_at	AHI1	Abelson helper integration site 1
-1.317	1374073_at	SLC46A1	solute carrier family 46 (folate transporter), member 1
-1.349	1387307_at	HAL*	histidine ammonia-lyase
-1.445	1397552_at	EML4	echinoderm microtubule associated protein like 4
-1.451	1387656_at	SLC4A1	solute carrier family 4 (anion exchanger), member 1 (Diego blood group)
-1.503	1393971_at	LOC102549203	uncharacterized LOC102549203
-1.658	1393910_at	Fam13a*	family with sequence similarity 13, member A
-1.736	1387052_at	GPT	glutamic-pyruvate transaminase (alanine aminotransferase)
-1.801	1368520_at	APOA4	apolipoprotein A-IV
-1.809	1387391_at	CDKN1A*	cyclin-dependent kinase inhibitor 1A (p21, Cip1)

* Interferon pathway transcript.

Table 3

Analysis of significant TBBPA liver transcripts and pathways (1000 mg/kg)*.

Ingenuity Canonical Pathways	-log(p-value)	Ratio	z-score	Molecules
Interferon Signaling	8.85E00	1.94E-01	2.449	OAS1,IRF9,STAT1,IFIT3,STAT2,ISG15,MX1
Activation of IRF by Cytosolic Pattern Recognition Receptors	4.47E00	7.94E-02	1.342	IRF9,IRF7,STAT1,STAT2,ISG15
Cell Cycle: G1/S Checkpoint Regulation	3.27E00	6.25E-02	-1.000	E2F6,GSK3B,CDKN1A,HDAC4
Cyclins and Cell Cycle Regulation	2.94E00	5.13E-02	NaN	E2F6,GSK3B,CDKN1A,HDAC4
Pancreatic Adenocarcinoma Signaling	2.46E00	3.77E-02	NaN	E2F6,RALBP1,STAT1,CDKN1A
Acetyl-CoA Biosynthesis III (from Citrate)	2.23E00	1E00	NaN	ACLY
Role of JAK1, JAK2 and TYK2 in Interferon Signaling	2.06E00	8.33E-02	NaN	STAT1,STAT2
Estrogen-mediated S-phase Entry	2.06E00	8.33E-02	NaN	E2F6,CDKN1A
JAK/Stat Signaling	2.06E00	4.17E-02	NaN	STAT1,STAT2,CDKN1A

* Analysis using ingenuity.com.